Neuroscience 227 (2012) 102–109

GLUTAMATE MODULATES RESTING STATE ACTIVITY IN THE PERIGENUAL ANTERIOR CINGULATE CORTEX – A COMBINED fMRI–MRS study

B. ENZI,[a] N. W. DUNCAN,[b] J. KAUFMANN,[c] C. TEMPELMANN,[c] C. WIEBKING[b] AND G. NORTHOFF[b]*

[a] *Department of Psychiatry, Psychotherapy and Preventive Medicine, LWL University Hospital Bochum, Ruhr-University Bochum, Bochum, Germany*

[b] *Mind, Brain Imaging and Neuroethics, Institute of Mental Health Research, University of Ottawa, Ottawa, Canada*

[c] *Department of Neurology, Otto-Von-Guericke University Magdeburg, Magdeburg, Germany*

Abstract—The perigenual anterior cingulate cortex (PACC) shows high resting state activity and is considered part of the default-mode network (DMN). However, the biochemical underpinnings of the PACC's high resting state activity remain unclear. While animal-based evidence points toward a role for the glutamatergic system, the modulation of the resting state activity level by itself as distinguished from stimulus-induced activity remains to be shown in humans. Using combined fMRI–MRS in healthy subjects, we here demonstrate that the PACC resting state concentration of glutamate is directly related to the level of resting state activity in the same region. In contrast, no such relationship could be detected during the anticipation of reward and punishment, nor in an independent control region (the left anterior insula). Taken together, our findings demonstrate for the first time the modulation of the PACC resting state activity level by the concentration of glutamate in the same regions. This contributes to a better understanding of the biochemical basis for the brain's resting state activity as well as providing some clues regarding its apparent pathological upregulation in psychiatric disorders like the major depressive disorder.

Key words: resting state, glutamate, perigenual anterior cingulate cortex, reward.

INTRODUCTION

Recent evidence from animal models, post-mortem studies, and challenge with the NMDA-antagonist Ketamine (Salvadore et al., 2009, 2010; Walter et al., 2009; Alcaro et al., 2010) indicate a potential role for glutamate in elevating resting state activity in the PACC. While these data provide indirect evidence for the role of glutamate in the modulation of the resting state activity level, direct evidence in healthy human subjects is still missing. In contrast to humans, there is a wide range of evidence from animals that resting state levels of glutamate and its respective receptors, (i.e., NMDA, AMPA and GluR2) impact the neural activity in the PACC (Millan, 2003; Johansen and Fields, 2004). Taken together with the well-known high density of glutamatergic receptors in the human PACC (Bozkurt et al., 2005; Palomero-Gallagher et al., 2008a,b), these data suggest that there may be a direct relationship between glutamate and the resting state activity level in the PACC in healthy subjects.

Human imaging studies have demonstrated the PACC to be part of the default-mode network (DMN), a group of regions that display high neuronal activity in the resting state (Raichle et al., 2001; Buckner et al., 2008). Among the regions of the DMN (medial prefrontal cortex, posterior cingulate cortex, hippocampus, lateral parietal cortex), the PACC seems to be special in that it shows a predominant deactivation in response to tasks. This means that tasks induce a negative BOLD response (NBR) within the region, rather than a positive BOLD response (PBR), with the NBR being broadly stimulus unspecific (Gusnard et al., 2001; Gusnard and Raichle, 2001; Northoff and Bermpohl, 2004; Northoff et al., 2007; Grimm et al., 2009). While NBR as a task-induced response has been associated with GABA in the PACC (Northoff et al., 2007), the biochemical modulation of the resting state activity level itself independent of its impact on NBR remains unclear. While recent studies (Duncan et al., 2011; Falkenberg et al., 2012) showed glutamate in PACC or SACC to modulate the transition from the resting state to stimulus-induced activity, i.e., rest–stimulus interaction (Northoff, 2012), it remains unclear whether the effects of glutamate are related to the resting state activity level by itself or its degree of modulation and change by the stimulus.

Major depressive disorder (MDD) is a debilitating psychiatric disorder that can be characterized by anhedonia. Anhedonia describes the inability to

*Corresponding author. Address: Canada Research Chair, Michael Smith Chair for Neuroscience and Mental Health, Research Unit Director, Mind, Brain Imaging and Neuroethics, Royal Ottawa Healthcare Group, University of Ottawa Institute of Mental Health Research, 1145 Carling Avenue, Room 6959, Ottawa, ON, Canada K1Z 7K4. Tel: +1-613-7226521x6801.

E-mail address: Georg.Northoff@theroyal.ca (G. Northoff).

Abbreviations: AN, anticipatory period for no-outcome; ANOVA, analysis of variance; AP, anticipatory period for punishment; AR, anticipatory period for reward; BSL, baseline events; Cr, to-creatine-ratio; DMN, default-mode network; GABA, gamma-aminobutyric acid; LAI, left anterior insula; MDD, major depressive disorder; MRS, magnetic resonance spectroscopy; NAA, *N*-acetylaspartate; NBR, negative BOLD response; PACC, perigenual anterior cingulate cortex; ROI, region of interest; SMA, supplementary motor area; VMPFC, ventromedial prefrontal cortex; VTA, ventral tegmental area.

0306-4522/12 $36.00
http://dx.doi.org/10.1016/j.neuroscience.2012.09.039

experience pleasure and has therefore been associated with changes in regions of the reward system including the ventral striatum (VS), the ventral tegmental area (VTA), the ventromedial prefrontal cortex (VMPFC) and the perigenual anterior cingulate cortex (PACC) (Steele et al., 2004; Heller et al., 2009; Pizzagalli et al., 2009; Eshel and Roiser, 2010; Hasler and Northoff, 2011). Among other regions, the PACC seems to be of significance for a deeper understanding of MDD since patients suffering from MDD show an abnormally elevated resting state activity in this region (Mayberg, 2003, 2009; Grimm et al., 2009; Alcaro et al., 2010; Price and Drevets, 2010; Northoff et al., 2011). In this regard, a better understanding of the functional and biochemical organization of the PACC in healthy subjects can provide more insight into the pathogenesis of MDD.

The aim of the current study was to investigate the relationship between the resting state level of glutamate and resting state- and stimulus-related signal changes in the PACC (as paradigmatic DMN region) of healthy subjects. To this end, we combined a well-established reward paradigm in fMRI, the Monetary Incentive Delay task (MID) (Knutson et al., 2001), with the measurement of PACC resting state concentration of glutamate in magnetic resonance spectroscopy (MRS) (Northoff et al., 2007; Walter et al., 2009). While the PACC as typical DMN region was the target region, we used the left anterior insula (LAI) as a control region that shows task-induced positive BOLD responses and is not part of the DMN (Buckner et al., 2008). Based on the animal- and receptor-based findings described above, we hypothesized that the PACC resting state concentration of glutamate in the healthy brain is specifically related to resting state-related signal changes rather than stimulus-induced activity, i.e., task-induced NBR, during reward in the PACC. Moreover, we assumed such correlation pattern between resting state-related signal changes and glutamate to not hold in the LAI, as this region is not part of the DMN.

EXPERIMENTAL PROCEDURES

Subjects

Nineteen healthy subjects with no psychiatric, neurological or medical illnesses were investigated (9 female, 10 male; average age 29.6 years, range 22–59 years; all right handed). The maximum BDI score in the investigated study sample was 5, indicating an absence of manifest depression. After a detailed explanation of the study design and potential risks, all subjects gave their written-informed consent. FMRI and MRS sessions were carried out on subsequent days in a randomized order. Participants had taken no medication or caffeine prior to either scanning session. These 19 subjects completed both fMRI and MRS. The study was approved by the institutional review board of the University of Magdeburg, Germany.

MRS data acquisition and analysis

Single-voxel 1H MR spectra were acquired during the resting state using a 3T whole body MRI system (Siemens Magnetom Trio) using an eight-channel head coil (PRESS, TR = 2 s; TE = 80 ms). Voxels were prescribed on a high-resolution T1-weighted 3D data set (MPRAGE, TR = 2 s; TI = 1.1 s; TE = 4.8 ms; flip angle = 7°; FoV = 256 × 256 × 192 mm; spatial resolution = 1 × 1 × 1 mm). One voxel of 20 × 10 × 20 mm was placed in the bilateral PACC, while a second was placed in the left anterior insula (LAI; 15 × 10 × 20 mm). Because of the crucial role of the PACC in the default mode network, we concentrated our correlation analysis on this region. Spectra were eddy current corrected and analyzed using LCModel version 6.1.0 (www.s-provencher.com/pages/lcmodel.shtml). Spectra with full-width-half-maximum line widths larger than 8 Hz and quantification results with a Cramér-Rao lower bound higher than 20% were excluded from further analysis. The measurements for two subjects in the PACC and one subject in the LAI were discarded for these reasons (PACC: n = 17; LAI: n = 18). Metabolite concentrations are given as their ratio to the measured creatine concentration. As a slight interdependence, due to a spectral overlap in their resonances, exists between quantification results for glutamate and glutamine these were quantified together. This combined concentration ratio of glutamate/glutamine to creatine is referred to henceforth as Glx.

Experimental paradigm

The fMRI scanning session was divided into four scanning runs. In the first functional run a well-established reward/punishment task was displayed. In the following three runs a modified reward task was presented, which will not be discussed in this article. Prior to entering the scanner all subjects completed a trial run of the tasks in order to familiarize them fully with the applied paradigm. In the scanner, images were displayed using the 'Presentation' software package (Neurobehavioural Systems, Albany, CA, USA), and were projected onto a screen visible through a mirror mounted on the headcoil via an LCD projector.

The reward/punishment task was a modified version of the monetary incentive delay task (Knutson et al., 2001), requiring the subject to press a button with the index finger of their right hand within a certain time of a target image (a black square in the center of the screen) being displayed. The length of this time period was determined in accordance with the average reaction time obtained in the pre-scan trial run, allowing the difficulty of the task to be modulated according to the individual's ability, and varied between 0.2 and 0.5 s. Furthermore, we wanted to ensure that in approximately 60% of all trials the required response was successful. Prior to this target image being displayed, a symbol indicating what the possible outcomes of the task would be – either reward, punishment, or no-outcome – was shown for 0.3 s, followed by a 2.25–2.75 s anticipation period. During the anticipation period a light-colored cross was displayed in the center of the screen.

In reward trials, completing the task successfully resulted in the subject winning €1, while failure meant that they would neither win nor lose anything. During punishment trials, a response within the required time period resulted in the subject neither winning nor losing money, while an unsuccessful response resulted in €1 being deducted from their total. Finally, in no-outcome trials no money was either won or lost, regardless of whether the subject responded within the required time period or not. Subjects were, however, instructed to still respond to the cue as quickly as possible. An equal number (30) of reward, punishment, and no outcome trials were displayed in each of the three reward/punishment runs in a pseudo-random order, giving a total of 90 instances of each trial type. Each trial was followed by a feedback stage during which the subject was informed of the outcome. The amount of money won or lost in the preceding trial was displayed, along with the running total for their winnings, for a period of 1.65 s. Trials were separated by a 4–5 s inter-trial interval, during

which the same light-colored cross as that shown during the anticipation period was displayed. The anticipatory period for reward (AR), punishment (AP) and no-outcome (AN) trials were included in our design matrix along with their respective feedback periods. In total, 24 baseline events (BSL) shown for 6–8 s were included in the design matrix to represent resting state activity. Baseline events were indicated by a light gray fixation cross, which was clearly distinguishable from the anticipation period and the inter trial interval (Duncan et al., 2011; Enzi et al., 2011).

fMRI data acquisition and analysis

The fMRI part of the study was carried out on a 1.5T MR scanner (General Electric Signa Horizon) using the standard circular polarized headcoil. Using a midsagittal scout image, a stack of 23 slices was aligned parallel to the bicomissural plane. During each functional run 320 whole brain volumes were acquired (gradient echo EPI, TR = 2 s; TE = 35 ms; flip angle = 80°; FoV = 200 × 200 mm^2; slice thickness = 5 mm, interslice gap = 1 mm, spatial resolution = 3.125 × 3.125 × 5 mm^3). Image processing and statistical analyses were carried out according to the general linear model approach (Friston et al., 1995) using the SPM5 software package (Wellcome Department of Imaging Neuroscience, London, UK) running on MATLAB 6.5.1 (The Mathwork Inc., Natick, MA, USA). The first five volumes were discarded due to saturation effects. All functional images were slice-time corrected with reference to the first slice acquired, corrected for motion artefacts by realignment to the first volume, and spatially normalized to a standard T1-weighted SPM template. The images were resampled to 2 × 2 × 2 mm^3 and smoothed with an isotropic 6-mm full-width half-maximum Gaussian kernel. The time-series fMRI data were filtered using a high-pass filter and cut-off of 128 s. A statistical model for each subject was computed by applying a canonical response function. We included the conditions anticipation of reward, punishment and no-outcome, their successful feedback (successful performance in reward trials, successful performance in punishment trials, successful performance in no-outcome trials) and the baseline event, resulting in seven conditions.

Regionally specific condition effects were tested by employing linear contrasts for each subject and each condition of interest. Since we were mainly interested in the so-called default mode network and its relation to reward anticipation, we concentrated the following second-level random effects analysis (one-sample *t*-test) on the contrast '[BSL] > [AR]'. The resulting statistical map was small-volume corrected with reference to the PACC MRS voxel (center of mass [MNI]: 0, 37, 2; extent: *x*: −10/10, *y*: 32/42, *z*: −8/12). For validation of our experimental paradigm, the contrast '[AR] > [AN]' was also calculated. Unless otherwise indicated all contrasts were FDR corrected (Genovese et al., 2002). To explore the anatomical localization of our correlation results, we calculated a SPM-based regression analysis between the PACC Glx/Cr level measured using MRS and the contrast '[BSL] > [AR]'. The results were small-volume corrected using (i) the PACC MRS voxel and (ii) the anatomically defined PACC ROI after gray-matter segmentation. Only activations surviving FWE correction were reported. The anatomical localization of significant activations was assessed with reference to the standard stereotactic atlas by superimposition on a standard brain template (Montreal Neurological Institute, MNI) provided by SPM5.

Since the PACC MRS voxel encompasses a volume of 4000 mm^3, an anatomically defined region of interest (ROI) located in the PACC (volume 1400 mm^3; center of mass [MNI]: 0, 37.1, −2.06; extent: *x*: −4/4, *y*: 32/42, *z*: −10/6; see Fig. 1A for the exact position in relation to the PACC MRS voxel) was defined using the WFU PickAtlas toolbox for SPM5 (Maldjian et al., 2003). The percent signal change for the above-mentioned PACC ROI was extracted using the MarsBar toolbox for SPM5 (http://marsbar.sourceforge.net) (Brett et al., 2002). All further statistical analysis (Pearson correlation, *t* test for paired variables) was carried out with the software package SPSS 11 (SPSS Inc., Chicago, USA).

In more detail, Pearson correlations between Glx/Cr derived from the same PACC ROI as that for which signal changes for our conditions of interest were extracted (i.e. [AR], [AP], [AN], [BSL], and the differences [BSL – AR], [BSL – AP] and [BSL – AN]) were calculated. Because of the the known age dependency of the PACC Glx level, all correlations were controlled for age as described by Gallinat et al. (2007). Furthermore, potential outliers were identified and excluded using the SPSS software. Outliers were defined following the definition of Walter et al. (2009).

As control region, the left anterior insula (LAI) was used. For this purpose, an anatomically defined ROI located in the LAI was defined as described previously (Enzi et al., 2009). Following the procedure outlined above, Glx/Cr values derived from the LAI MRS voxel were correlated with the percent signal change derived from the same region.

RESULTS

Signal changes in fMRI

We first calculated the contrast '[AR] > [AN]' to show that our reward paradigm yielded activity in the reward system. As expected, we observed an activation pattern consistent with previous studies, including the bilateral ventral striatum, the left putamen, the left anterior cingulate, the left anterior insula, the left supplementary motor area (SMA), and the bilateral ventral tegmental area (VTA) (Fig. 3 and Table 2).

In addition, the contrast '[BSL] > [AR]' (with small-volume correction for the PACC MRS voxel) revealed an activation located in the PACC (MNI: 2, 36, 0) (Fig. 1C). A more fine-grained analysis concerning the differentiation between [AR] and [BSL], and [AN] and [BSL], revealed task-induced deactivations in relation to the baseline condition observable in the anatomically defined PACC ROI (Fig. 1B).

MRS results

The metabolite levels in terms of the to-creatine-ratio (Cr) derived from the PACC voxel were as follows (mean, ±SD): *N*-acetylaspartate/Cr: 1.18 (±0.11); Choline/Cr: 0.22 (±0.02); Glx/Cr: 1.28 (±0.17); myo-inositol: 0.76 (±0.15).

In the LAI, metabolite levels were 1.4 (±0.21) for *N*-acetylaspartate/Cr, 0.21 (±0.02) for choline/Cr, 1.37 (±0.27) for Glx/Cr, and 0.63 (±0.13) for myo-inositol.

Correlation analysis between Glx/Cr and fMRI

We calculated the correlation between Glx/Cr and the percent signal change for the condition of interest (i.e., [AR], [AP], [AN], [BSL – AR], [BSL – AP] and [BSL – AN]. The fMRI signal change was extracted using an anatomically defined ROI encompassing the bilateral PACC. We were able to detect a significant positive correlation (partial correlation controlled for age after exclusion of outliers; the exact number of included cases is given in Table 1) between Glx/Cr and [BSL]

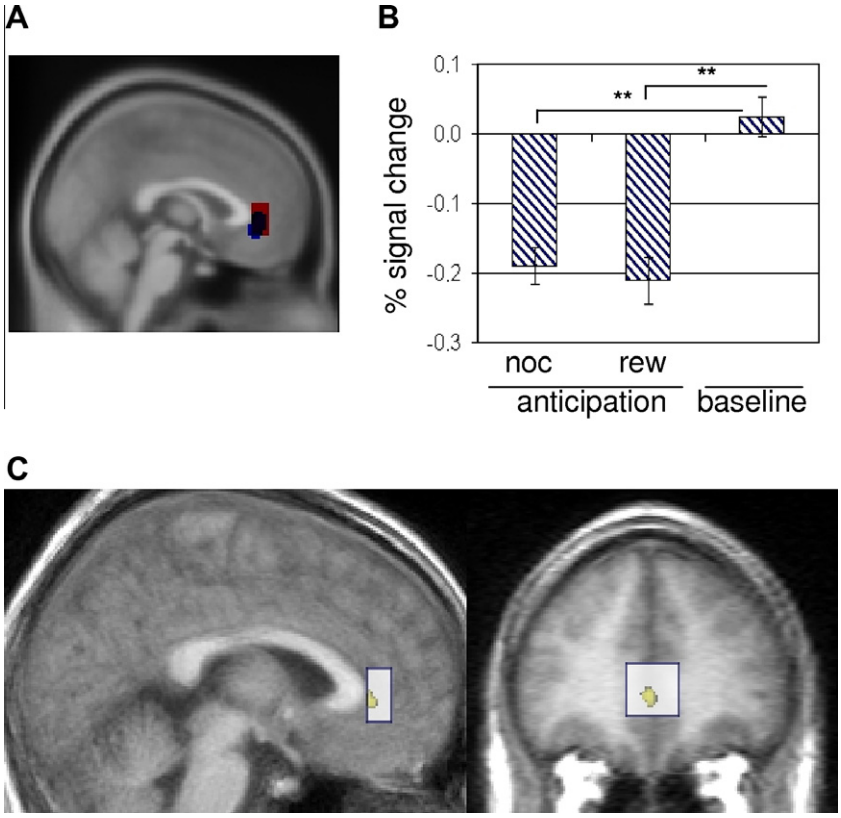

Fig. 1. (A) Position of the anatomically defined region of interest (ROI) used for percent signal change extraction (blue) in relation to the MRS voxel (red) placed in the pregenual anterior cingulate cortex (PACC). (B) Percent signal change for the conditions 'anticipation of no outcome', 'anticipation of reward', and 'baseline' derived from the above-mentioned anatomically defined ROI placed in the PACC. $^{**}p < 0.01$; Error bar = S.E.M. (C) Contrast 'baseline > anticipation of reward' (p[FDR] < 0.05; $k > 10$) with Small-Volume Correction for the MRS voxel placed in the PACC. (For interpretation of the references to color in this figure legend, the reader is referred to the web version of this article.)

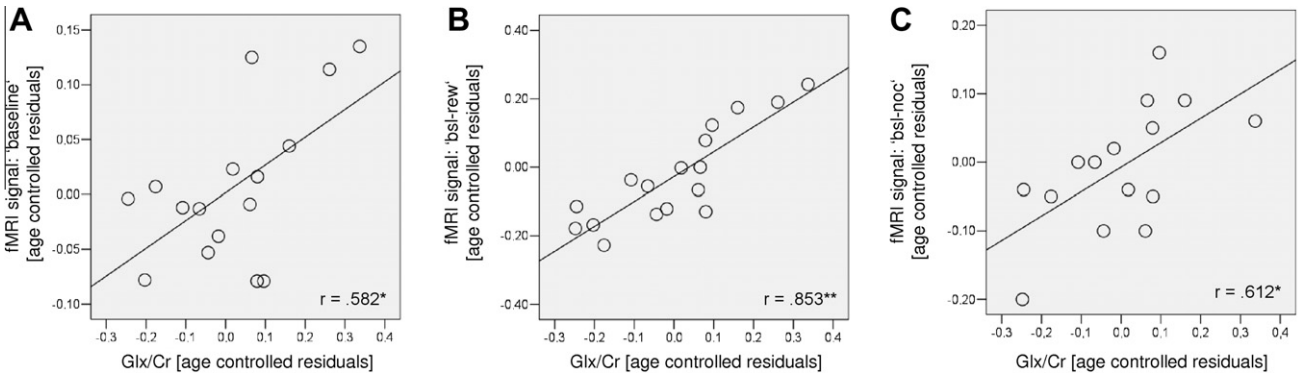

Fig. 2. Pearson-correlation between the Glx/Cr-ratio derived from the MRS voxel located in the PACC and the fMRI signal for the conditions (A) 'baseline', (B) 'baseline – anticipation of reward', and (C) 'baseline – anticipation of no outcome'. It should be noted, that values can be negative as they represent residuals after linear correction for age.

(rPearson = .582*), Glx/Cr and [BSL – AR] (rPearson = .853**), and Glx/Cr and [BSL – AN] (rPearson = .612*), whereas concerning all other contrasts, non-significant results were obtained (Table 1, Fig. 2). In addition, no significant correlations between the Glx/Cr level in the LAI and above-mentioned conditions were observed (Table 1).

The SPM-based regression analysis between the PACC Glx/Cr-ratio measured using MRS and the contrast '[BSL] > [AR]' confirmed the results outlined above and localized the correlation to the left PACC (MNI coordinates: −4, 36, −4; p[FWE with S.V.C. for MRS voxel] = 0.005, $t_{15} = 6.28$) (Fig. 3B). These results were confirmed by a second SPM-based regression analysis after gray-matter segmentation of the anatomically defined PACC ROI (MNI coordinates: −4, 34, −4; p[FWE with S.V.C.] < 0.001, $t_{15} = 6.88$) (Fig. 3B).

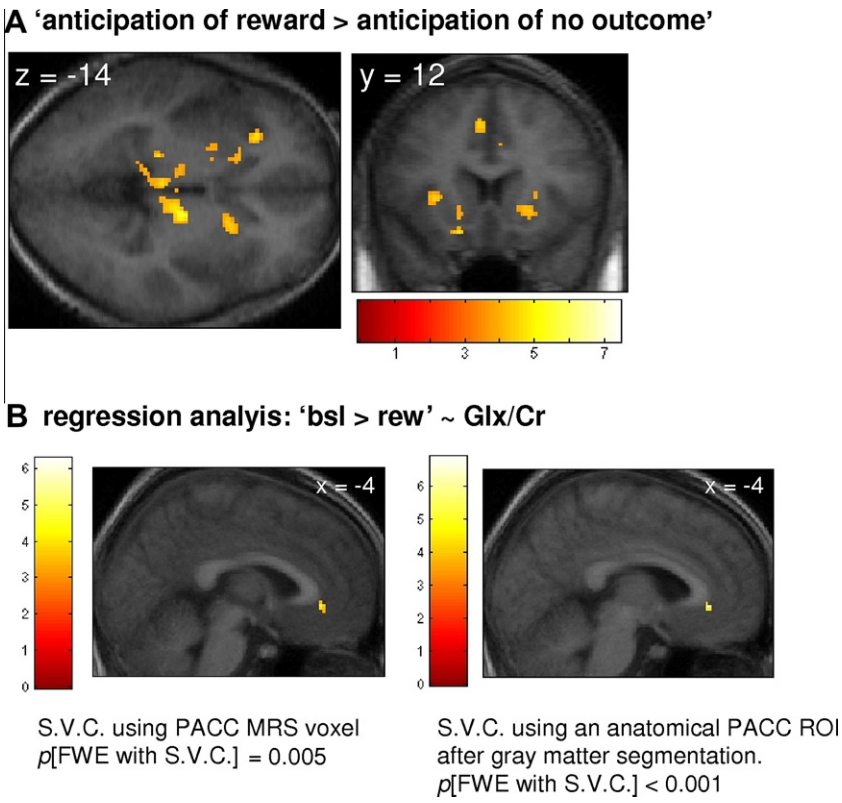

Fig. 3. (A) SPM contrast 'anticipation of reward > anticipation of no outcome' calculated using a threshold of p[FDR] < 0.05 for an extent k > 20 voxel. (B) SPM-based regression analysis between the PACC Glx/Cr-ratio measured using MRS and the contrast 'baseline – anticipation of reward'. Small-volume correction was applied using (i) the PACC MRS voxel, and (ii) an anatomically defined PACC after segmentation. Only activations surviving a threshold of p[FWE] < 0.05 for an extent of k > 5 voxel were reported.

Table 1. Pearson-correlations between [Glx/Cr] and the fMRI signal change

Region	Condition	$r_{Pearson}$	p[a]	n[b]
PACC[a]	Baseline	.582	0.018	16
	Anticipation of reward	−.296	0.266	16
	Anticipation of punishment	−.436	0.092	16
	Anticipation of no outcome	−.204	0.432	17
	Baseline – anticipation of reward	.853	< 0.001	17
	Baseline – anticipation of punishment	.255	0.340	16
	Baseline – anticipation of no outcome	.612	0.015	15
Left anterior insula[b]	Baseline	.06	0.868	17
	Anticipation of reward	.090	0.721	18
	Anticipation of punishment	.053	0.841	17
	Anticipation of no outcome	−.175	0.503	17
	Baseline – anticipation of reward	.022	0.937	18
	Baseline – anticipation of punishment	−.357	0.175	16
	Baseline – anticipation of no outcome	−.106	0.675	16

[a] p-Value, two-sided.
[b] Number of included cases after correction for outliers.

In order to obtain regions associated with the default-mode network (DMN), we, in a second step, calculated a one-way ANOVA with the contrasts '[BSL] > [AR]', '[BSL] > [AP]' and '[BSL] > [AN]' and the main factor 'positive effect of condition'. This yielded signal changes in the typical regions of the DMN including the bilateral PACC, the dorsomedial prefrontal cortex (DMFC), the precuneus, and the bilateral superior temporal gyrus (see Table 1). Since the PACC was our target region here, we extracted signal changes from right and left PACC in the respective coordinates that were significant in the ANOVA; it should also be mentioned that both coordinates as yielded in the ANOVA were lying within the voxel we employed in MRS to measure Glutamate in the PACC (see Fig. 1). As expected, the bilateral PACC showed negative signal changes (NBR) during both the anticipation and the feedback period. This deactivation was stronger during the anticipation period

Table 2. Activations in response to the contrast 'anticipation of reward > anticipation of no outcome'

Region	Co-ordinates [MNI]	*t*-Value	*z*-Value
Left ventral striatum	−18, 6, −16	4.31	3.53
Right ventral striatum	20, 14, −4	4.49	3.63
Left putamen	−26, 6, −10	4.90	3.86
Left anterior insula	−32, 30, −4	4.66	3.72
Left insula	−32, 14, 2	4.94	3.88
Left dorsomedial thalamus	−4, −22, −2	5.05	3.93
Right dorsomedial thalamus	14, −16, −2	5.68	4.24
Left VTA	−6, −30, −12	7.01	4.81
Right VTA	4, −30, −10	4.23	3.48
Left anterior cingulate	−6, 32, 18	5.33	4.07
Left SMA	−2, −12, 62	5.44	4.13
Left parietal cortex	−38, −40, 56	5.56	4.19
Right parietal cortex	34, −20, 42	7.45	4.97
Right temporoparietal junction	48, −22, −6	5.41	4.12
Left VLPFC	−22, 48, 4	4.67	3.73

Initial threshold p(FDR) < 0.05, k > 20 voxel.
Abbreviations: SMA: supplementary motor area; VLPFC: ventrolateral prefrontal cortex; VTA: ventral tegmental area.

than in the feedback period (see Fig. 1). In contrast, negative signal changes were not observed in the baseline, fixation cross, period (Fig. 1).

DISCUSSION

Our combined fMRI–MRS investigation demonstrates a close relationship between glutamate and resting state activity level in the PACC. More specifically, we were able to show that the resting state concentration of glutamate in the PACC is positively related to the level of resting state activity, as measured during the task fixation period, in the same region. In addition, the differences between this resting state level and the above-mentioned conditions correlate positively with the glutamate level in the PACC. This pattern was specific to the PACC, a typical DMN region, but was not observed in the left anterior insula, as task-positive region not considered part of the DMN. Our findings thus provide evidence for the glutamatergic modulation of PACC resting state activity levels in the healthy brain.

Our fMRI results showed stimulus-induced negative BOLD responses in the PACC during reward anticipation. This is in accordance with previous findings that show the stimulus-nonspecific nature of NBR in this region (Gusnard et al., 2001; Gusnard and Raichle, 2001; Northoff and Bermpohl, 2004; Northoff et al., 2007; Grimm et al., 2009). This is assumed to reflect the high resting state activity in this region that has led to it being described as part of the DMN (Raichle et al., 2001; Buckner et al., 2008). In this context, the PACC must be distinguished from regions not belonging to the DMN like the (left) anterior insula that show (task-induced) positive BOLD responses.

A recent study by Falkenberg et al. (2012) investigated the relationship between glutamate levels in the dorsal ACC (dACC) and the BOLD response evoked by a task requiring cognitive control. The authors demonstrated that subjects expressing a low glutamate level in dACC showed a higher BOLD response in the inferior parietal lobe, the orbitofrontal cortex, the retrosplenial cortex, and the basal ganglia when the task required a high level of cognitive control. In contrast to this finding, high-glutamate subjects showed the opposite relationship with enhanced BOLD response in the same regions under low cognitive control (Falkenberg et al., 2012). Because of the known involvement of glutamate in the brain's energy turnover (for review see Mangia et al., 2009) the results of the present study, as well as the results of Falkenberg et al. (2012), can be interpreted as an up-regulation of resting-state activity mediated by glutamate.

It should be noted, that the voxel used for 1H-MRS by Falkenberg et al. (2012) was located in the (anterior-)dorsal ACC (Etkin et al., 2011), a region commonly associated with various cognitive functions, whereas in the present study the spectroscopic measurement of glutamate was carried out in the perigenual ACC (PACC), i.e. the 'affective' subdimension of the anterior cingulate (Bush et al., 2000). Although this concept of the ACC organization and function was very popular, the exact functional organization of the ACC is still a matter of debate (for review see Etkin et al., 2011; Shackman et al., 2011). Moreover, the anterior-dorsal ACC and PACC show, at least partly, an overlapping pattern of connectivity with various limbic regions (e.g. the amygdala, the periacqueductal gray, and the hypothalamus) supporting the notion of the ACC as an integrative structure (Etkin et al., 2011).

In addition, the level of glutamatergic activity is not only related to the resting state activity, but has also direct implications for deactivations during task performance, i.e. the difference between resting state and task-related conditions (Duncan et al., 2011). In this regard, the concept of ''rest–stimulus interaction'' (Northoff et al., 2010) is supported by our data.

Our findings are compatible with recent observations in non-human animals, where glutamate has been shown to modulate resting state activity levels in the PACC, (Millan, 2003; Johansen and Fields, 2004). Moreover, our findings fit in with cytoarchitectonic results that show a high level of glutamatergic receptors (NMDA, AMPA and GluR2) in the human PACC (Bozkurt et al., 2005; Palomero-Gallagher et al., 2008a,b).

Finally, our findings may open the door toward a better understanding of the abnormally elevated resting state activity in MDD. Since glutamate is a predominantly excitatory transmitter, our finding of increased Glutamate levels going along with increased resting state activity levels suggests that such neural excitation plays a role in maintaining the resting state activity level. one could thus hypothesize that the above-described neural excitation may be abnormally high in MDD, leading to the abnormally elevated resting state activity levels and glutamatergic hyperfunction observed in these patients (Salvadore et al., 2009, 2010; Walter et al., 2009; Alcaro et al., 2010; Banasr et al., 2010; Price and Drevets, 2010; Hasler and Northoff, 2011; Northoff et al., 2011). The reasons behind such glutamatergic hyperfunction and its apparently abnormal upregulation of the resting state activity level remain unclear, however, and need to be addressed in future studies (see Banasr et al., 2010, for one step in this direction). The relationship between PACC glutamate and task-induced negative BOLD response (NBR) in MDD was investigated by a recent imaging study. Walter et al. (2009) demonstrated a correlation between PACC glutamate and *N*-acetylaspartate (NAA) levels and NBR induced by an emotional fMRI task. In addition, glutamate and NAA levels correlated with emotional intensity ratings that could serve as a surrogate marker for anhedonia (Walter et al., 2009). The authors speculate that this altered PACC function in MDD is probably related to an altered resting state activity in the very same region.

Limitations

Several limitations of our study need to be mentioned. First, the resting state period used in this study was rather short, although clearly distinguishable from the anticipation period and the inter-trial interval. Due to the fact that it was interspersed between the different experimental conditions, it can only be considered to be an approximation of a 'true' resting state condition. Second, one may question the biochemical specificity of our findings since we did not include γ-aminobutyric acid in the MRS session. A recent study demonstrated the relationship between NBR and GABA during task-induced responses in the PACC (Northoff et al., 2007). In contrast to our current findings, GABA was not related to the signal changes during the resting state itself but only to the task-related deactivation (Northoff et al., 2007). In this context, Falkenberg et al. (2012) speculate that both neurotransmitters, i.e. glutamate and GABA, contribute to the ''individual variations in the BOLD response''. This suggests that GABA may be crucial in mediating the transition from the resting state to stimulus-induced activity, while glutamate may maintain the activity level of the resting state itself. However, this hypothesis remains speculative and must be demonstrated in future studies combining the measurement of both GABA and glutamate. Furthermore, we concentrated our ROI analysis on the PACC as a ''key region'' of the default mode network. Relying on the current literature (Duncan et al., 2011; Falkenberg et al., 2012) it is likely that the glutamate concentration measured in the PACC, or – more specifically – the glx-level, has an influence on other regions of the default mode network. However, since we did not investigate the influence of the PACC Glx/Cr-level on the connectivity pattern of the default mode network, this interpretation of our results remains speculative and must be verified in future studies.

In the present study, the combined signal for glutamate and glutamine (glx) was measured for technical reasons. The combined glx signal reflects complex physiological processes located in astroglial cells and neurons (for review see Javitt et al., 2011). For this reason, further evidence is needed regarding the exact relationship between the PACC glutamate concentration and the baseline activity in the very same region.

CONCLUSIONS

In conclusion, we here demonstrate for the first time the glutamatergic modulation of the level of resting state activity in the PACC of healthy subjects. Our findings indicate that glutamatergic-mediated neural excitation may be crucial in maintaining the resting state activity level in the PACC, as opposed to mediating the modulation of the resting state by the stimulus. These findings not only shed novel light on the biochemical modulation of neural activity in the DMN but are also highly relevant for understanding the abnormalities in the PACC and the DMN in psychiatric disorders like depression.

Acknowledgments—The authors would like to thank M. de Greck for his invaluable help with the study design and analysis, D. Hayes for his useful comments, and E. Stockum and C. Ulrich for their assistance with the recruitment of subjects and conducting of scanning sessions. Thanks also to the staff at the Department of Neurology for their skilful assistance. The work was supported by grants to G.N. from the Hope of Depression Research Foundation (HDRF), German Research Foundation DFG/SFB 776 A6, the EJLB Michael Smith Foundation, and CRC Canada Research Chair.

REFERENCES

Alcaro A, Panksepp J, Witczak J, Hayes DJ, Northoff G (2010) Is subcortical-cortical midline activity in depression mediated by glutamate and GABA? A cross-species translational approach. Neurosci Biobehav Rev 34:592–605.

Banasr M, Chowdhury GM, Terwilliger R, Newton SS, Duman RS, Behar KL, et al (2010) Glial pathology in an animal model of depression: reversal of stress-induced cellular, metabolic and behavioral deficits by the glutamate-modulating drug riluzole. Mol Psychiatry 15:501–511.

Bozkurt A, Zilles K, Schleicher A, Kamper L, Arigita ES, Uylings HB, Kötter R (2005) Distributions of transmitter receptors in the macaque cingulate cortex. NeuroImage 25:219–229.

Brett M, Anton J-L, Valabregue R, Poline J-B (2002) Region of interest analysis using an SPM toolbox. 8th International conference on functional mapping of the human brain, Sendai, Japan. NeuroImage 16.

Buckner RL, Andrews-Hanna JR, Schacter DL (2008) The brain's default network: anatomy, function, and relevance to disease. Ann N Y Acad Sci 1124:1–38.

Bush G, Luu P, Posner MI (2000) Cognitive and emotional influences in anterior cingulate cortex. Trends Cogn Sci 4:215–222.
Duncan NW, Enzi B, Wiebking C, Northoff G (2011) Involvement of glutamate in rest–stimulus interaction between perigenual and supragenual anterior cingulate cortex: a combined fMRI–MRS study. Hum Brain Mapp 32:2172–2182.
Enzi B, de Greck M, Prösch U, Tempelmann C, Northoff G (2009) Is our self nothing but reward? Neuronal overlap and distinction between reward and personal relevance and its relation to human personality. PlosOne 4:e8429.
Enzi B, Doering S, Faber C, Hinrichs J, Bahmer J, Northoff G (2011) Reduced deactivation in reward circuitry and midline structures during emotion processing in borderline personality disorder. World J Biol Psychiatry [Epub ahead of print].
Eshel N, Roiser JP (2010) Reward and punishment processing in depression. Biol Psychiatry 68:118–124.
Etkin A, Egner T, Kalisch R (2011) Emotional processing in anterior cingulate and medial prefrontal cortex. Trends Cogn Sci 15:85–93.
Falkenberg LE, Westerhausen R, Specht K, Hugdahl K (2012) Resting-state glutamate level in the anterior cingulate predicts blood–oxygen level-dependent response to cognitive control. Proc Natl Acad Sci USA 109:5069–5073.
Friston KJ, Holmes A, Worsley K, Poline JB, Frith C, Frackowiak RSJ (1995) Statistical parametric maps in functional imaging: a general linear approach. Hum Brain Mapp 2:189–210.
Gallinat J, Kunz D, Lang UE, Neu P, Kassim N, Kienast T, Seifert F, Schubert F, Bajbouj M (2007) Association between cerebral glutamate and human behaviour: the sensation seeking personality trait. NeuroImage 34:671–678.
Genovese C, Lazar N, Nichols T (2002) Thresholding of statistical maps in functional neuroimaging using the false discovery rate. NeuroImage 15:870–878.
Grimm S, Boesiger P, Beck J, Schuepbach D, Bermpohl F, Walter M, Ernst J, Hell D, Boeker H, Northoff G (2009) Altered negative BOLD response in the default moder network during emotion processing in depressed subjects. Neuropsychopharmacology 34:932–943.
Gusnard DA, Raichle ME (2001) Searching for a baseline: functional imaging and the resting human brain. Nat Rev Neurosci 2:685–694.
Gusnard DA, Akbudak E, Shulman GL, Raichle ME (2001) Medial prefrontal cortex and self-referential mental activity: relation to a default mode of brain function. Proc Natl Acad Sci USA 98:4259–4264.
Hasler G, Northoff G (2011) Discovering imaging endophenotypes for major depression. Mol Psychiatry 16:604–619.
Heller AS, Johnstone T, Shackman AJ, Light SN, Peterson MJ, Kolden GG, Kalin NH, Davidson RJ (2009) Reduced capacity to sustain positive emotion in major depression reflects diminished maintenance of fronto-striatal brain activation. Proc Natl Acad Sci USA 106:22445–22450.
Javitt DC, Schoepp D, Kalivas PW, Volkow ND, Zarate C, Merchant K, Bear MF, Umbricht D, Hajos M, Potter WZ, Lee CM (2011) Translating glutamate: from pathophysiology to treatment. Sci Transl Med 28:102mr2.
Johansen J, Fields H (2004) Glutamatergic activation of anterior cingulate cortex produces an aversive teaching signal. Nat Neurosci 7:398–403.
Knutson B, Adams CM, Fong GW, Hommer D (2001) Anticipation of increasing monetary reward selectively recruits nucleus accumbens. J Neurosci 21:RC159.
Maldjian JA, Laurienti PJ, Kraft RA, Burdette JH (2003) An automated method for neuroanatomic and cytoarchitectonic atlas-based interrogation of fMRI data sets. NeuroImage 19:1233–1239.
Mangia S, Giove F, Tkác I, Logothetis N, Henry P, Olman C, Maraviglia B, Di Salle F, Uqurbil K (2009) Metabolic and hemodynamic events after changes in neuronal activity: current hypotheses, theoretical predictions and *in vivo* NMR experimental findings. J Cereb Blood Flow Metab 29:441–463.
Mayberg HS (2003) Positron emission tomography imaging in depression: a neural systems perspective. Neuroimaging Clin N Am 13:805–815.
Mayberg HS (2009) Targeted electrode-based modulation of neural circuits for depression. J Clin Invest 119:717–725.
Millan M (2003) The neurobiology and control of anxious states. Prog Neurobiol 70:83–244.
Northoff G (2012) Psychoanalysis and the brain – why did freud abandon neuroscience? Front Psychol 3:71.
Northoff G, Bermpohl F (2004) Cortical midline structures and the self. Trends Cogn Sci 8:102–107.
Northoff G, Walter M, Schulte RF, Beck J, Dydak U, Henning A, Boeker H, Grimm S, Boesiger P (2007) GABA concentrations in the human anterior cingulate cortex predict negative BOLD response in fMRI. Nat Neurosci 10:1515–1517.
Northoff G, Qin P, Nakao T (2010) Rest–stimulus interaction in the brain: a review. Trends Neurosci 33:277–284.
Northoff G, Wiebking C, Feinberg T, Panksepp J (2011) The 'resting-state hypothesis' of major depressive disorder – a translational subcortical-cortical framework for a system disorder. Neurosci Biobehav Rev 35:1929–1945.
Palomero-Gallagher N, Mohlberg H, Zilles K, Vogt B (2008a) Cytology and receptor architecture of human anterior cingulate cortex. J Comp Neurol 508:906–926.
Palomero-Gallagher N, Vogt B, Schleicher A, Mayberg HS, Zilles K (2008b) Receptor architecture of the human cingulate cortex: evaluation of the four-region neurobiological model. Hum Brain Mapp 30:2336–2355.
Pizzagalli DA, Holmes AJ, Dillon DG, Goetz EL, Birk JL, Bogdan R, Dougherty DD, Iosifescu DV, Rauch SL, Fava M (2009) Reduced caudate and nucleus accumbens response to rewards in unmedicated individuals with major depressive disorder. Am J Psychiatry 166:702–710.
Price JL, Drevets WC (2010) Neurocircuitry of mood disorders. Neuropsychopharmacology 35:192–216.
Raichle ME, MacLeod AM, Snyder AZ, Powers WJ, Gusnard DA, Shulman GL (2001) A default mode of brain function. Proc Natl Acad Sci USA 98:676–682.
Salvadore G, Cornwell BR, Colon-Rosario V, Coppola R, Grillon C, Zarate Jr CA, Manji HK (2009) Increased anterior cingulate cortical activity in response to fearful faces: a neurophysiological biomarker that predicts rapid antidepressant response to ketamine. Biol Psychiatry 65:289–295.
Salvadore G, Cornwell BR, Sambataro F, Latov D, Colon-Rosario V, Carver F, Holroyd T, DiazGranados N, Machado-Vieira R, Grillon C, Drevets WC, Zarate Jr CA (2010) Anterior cingulate desynchronization and functional connectivity with the amygdala during a working memory task predict rapid antidepressant response to ketamine. Neuropsychopharmacology 35:1415–1422.
Shackman AJ, Salomons TV, Slagter HA, Fox AS, Winter JJ, Davidson RJ (2011) The integration of negative affect, pain and cognitive control in the cingulate cortex. Nat Rev Neurosci 12:154–167.
Steele JD, Meyer M, Ebmeier KP (2004) Neural predictive error signal correlates with depressive illness severity in a game paradigm. NeuroImage 23:269–280.
Walter M, Henning A, Grimm S, Schulte RF, Beck J, Dydak U, Schnepf B, Boeker H, Boesiger P, Northoff G (2009) The relationship between aberrant neuronal activation in the pregenual anterior cingulate, altered glutamatergic metabolism, and anhedonia in major depression. Arch Gen Psychiatry 66:478–486.

(Accepted 18 September 2012)
(Available online 25 September 2012)